Click Here for Full Article

Comparison of soil moisture dynamics between a tropical rain forest and a tropical seasonal forest in Southeast Asia: Impact of seasonal and year-to-year variations in rainfall

Tomo'omi Kumagai,[1] Natsuko Yoshifuji,[1] Nobuaki Tanaka,[2] Masakazu Suzuki,[3] and Tomonori Kume[1,4]

Received 24 July 2008; revised 25 December 2008; accepted 19 February 2009; published 14 April 2009.

[1] We examined the impact of both seasonal and year-to-year variations in precipitation on simulated soil moisture dynamics at a tropical rain forest (TRF) site and a tropical seasonal forest (TSF) site in Southeast Asia, between which there is a clear difference in the precipitation regime, through a probabilistic ecohydrological model. All model parameters have apparent physical meaning and were obtained by field observations. Rainfall statistics as the primary model forcing terms were constructed from long-term rainfall records, and their analysis revealed a close relationship between drought and El Niño events at the TRF site and a long-term drying trend at the TSF site. The model results further demonstrated that the studied ecosystem's robustness (mainly concerning the plant water availability) are attributed to functional factors such as soil texture for the TRF site and rooting depth and the dry season use of water from the preceding wet season for the TSF site.

Citation: Kumagai, T., N. Yoshifuji, N. Tanaka, M. Suzuki, and T. Kume (2009), Comparison of soil moisture dynamics between a tropical rain forest and a tropical seasonal forest in Southeast Asia: Impact of seasonal and year-to-year variations in rainfall, *Water Resour. Res.*, *45*, W04413, doi:10.1029/2008WR007307.

1. Introduction

[2] Tropical forests exist in a broad band girdling the Earth's moist equatorial regions and cover about 35% of the global forest area [*Food and Agricultural Organization of the United Nations*, 2005; *World Resources Institute*, 2007]. These forests receive high radiative energy, play a significant role in the global carbon budget [e.g., *Melillo et al.*, 1993; *Field et al.*, 1998; *Malhi and Grace*, 2000] and are a major source of global hydrologic fluxes with profound influences on both global and regional climates [e.g., *Lean and Warrilow*, 1989; *Nobre et al.*, 1991; *Kanae et al.*, 2001]. Although tropical forests in Southeast Asia (SEA) represent about 11% of the world's tropical forests in terms of area [*World Resources Institute*, 2007], the impact of these forests, which have the highest relative deforestation rate in tropical areas (e.g., relative clearance area to forested area 1990–1995: 0.6, 0.7 and 1.1% year^{-1} in the Americas, Africa and Asia, respectively) [*Houghton and Hackler*, 1999; *Laurance*, 1999; *Malhi and Grace*, 2000], on the global and regional climate and hydrological cycling is an important concern [e.g., *Kanae et al.*, 2001; *Malhi and Wright*, 2004; *Mabuchi et al.*, 2005a, 2005b].

[3] The tropics of SEA can be generally classified into two regions in terms of the seasonal variations in precipitation [see *Kumagai et al.*, 2005, Figure 3]: weak and strong seasonalities correspond to the regions of tropical rain forest (TRF) and tropical seasonal forest (TSF), respectively. While there is a clear difference between wet and dry seasons in the TSF region, the precipitation in the TRF region is abundant throughout the year [e.g., *Kumagai et al.*, 2005; *Yoshifuji et al.*, 2006; *Tanaka et al.*, 2008] although in some equatorial regions of SEA the amplitude of the seasonal cycle of precipitation was reported to be larger than the interannual variation [e.g., *Chappell et al.*, 2001]. Furthermore, an analysis of climatic trends of global TRF regions over the period 1960–1998 showed that rainfall appears to have declined more significantly in SEA than in Amazonia, and that the El Niño–Southern Oscillation (ENSO) is the primary driver inducing drought in SEA [*Malhi and Wright*, 2004]. In addition, a close relationship between the interannual variations of the monsoon onset and ENSO on the Indochina Peninsula was identified, and ENSO appears to be related to late monsoon onset leading to a reduction in annual precipitation [*Zhang et al.*, 2002].

[4] Therefore, it is logical to expect that the hydrological, atmospheric and ecological processes involving the soil–plant–atmosphere continuum (SPAC) in TRF and TSF in SEA respond to the intra (seasonal) and interannual (ENSO-related) variations in rainfall in these forest regions, respectively. Furthermore, the current trends in climatic factors for each of these forest regions affects each of the forest ecosystem processes such as water, energy and nutrient cycles. It should also be noted that quantifying and predicting hydrologic fluxes are prerequisites for describing a forest ecosystem process, and that soil moisture dynamics

[1]Kasuya Research Forest, Kyushu University, Sasaguri, Japan.
[2]University Forest in Aichi, Graduate School of Agriculture and Life Sciences, University of Tokyo, Seto, Japan.
[3]Graduate School of Agricultural and Life Sciences, University of Tokyo, Tokyo, Japan.
[4]Now at School of Forestry and Resource Conservation, National Taiwan University, Taipei, Taiwan.

Copyright 2009 by the American Geophysical Union.
0043-1397/09/2008WR007307$09.00

is a key factor controlling hydrologic fluxes through the SPAC [see *Rodríguez-Iturbe et al.*, 2001; *Laio et al.*, 2001a, 2001b; *Porporato et al.*, 2001, 2002; *Rodríguez-Iturbe and Porporato*, 2004].

[5] In this study, we analyze the statistical structure of the precipitation regimes and their resultant soil moisture dynamics in a Bornean TRF and a Thai TSF. We use an ecohydrological model to find a probabilistic description of soil moisture dynamics [*Laio et al.*, 2001b] taking into consideration the intra [*Miller et al.*, 2007] and interannual [*D'Odorico et al.*, 2000] rainfall fluctuation characteristics. For parameter estimation and validation, the observations from previous studies conducted in a Bornean TRF [*Kumagai et al.*, 2004a, 2004b, 2005] and a Thai TSF [*Tanaka et al.*, 2003, 2004] are used. In addition, long-term rainfall records collected in these regions are available as the main input for model calculations. Probabilistic description of soil moisture dynamics is thought to be useful for describing the effect of rainfall interannual variability on vegetation dynamics [e.g., *Borgogno et al.*, 2007]. Thus, the outcome of this study will be used to elucidate forest ecosystem processes and dynamics in the tropics of SEA, which are controlled in part by severe drought induced by ENSO cycles [e.g., *Nakagawa et al.*, 2000].

2. Theory

[6] The probabilistic soil moisture model used in this study was originally proposed by *Rodríguez-Iturbe et al.* [1999] and improved by *Laio et al.* [2001b]. A review and description of the modeling scheme is presented below for completeness. Note that *Rodríguez-Iturbe and Porporato* [2004] have provided more detailed information.

[7] The model provides a realistic and quantitative description of the temporal soil moisture dynamics and at the same time retains a level of simplicity amenable to analytical solution. As *Rodríguez-Iturbe and Porporato* [2004] stated, such an analysis is the necessary starting point for quantitative understanding of the impacts of soil moisture on ecosystem dynamics.

2.1. Soil Moisture Balance at a Point

[8] Under the conditions that lateral movement can be neglected, the vertically integrated soil moisture balance equation is given by

$$nZ_r \frac{ds(t)}{dt} = \varphi[s(t), t] - \chi[s(t)], \tag{1}$$

where n is the soil porosity, Z_r is the rooting depth, s is the degree of saturation varying between 0 and 1, t is time, φ is the rate of infiltration into the rooting zone, which is represented by the rainfall rate minus the rate of rainfall lost through canopy interception loss and the rate of infiltration excess, and χ is the rate of the water loss from the soil; i.e., the evapotranspiration rate $E[s(t), t]$ and the leakage $L[s(t)]$. Equation (1) is a stochastic ordinary differential equation for the state variable s, and solved on daily timescales.

2.2. Rainfall Infiltrating Into the Ground

[9] The frequency of rainfall events can be assumed to be a stochastic variable expressed as an exponential distribution with the mean time interval between precipitation events $1/\lambda$. The amount of rainfall, when rainfall occurs, is also assumed to be an independent random variable described by an exponential probability distribution with the mean depth of rainfall events α. Losses to the atmosphere from canopy interception are represented using a threshold of rainfall depth Δ, which denotes interception capacity and below which effectively no water reaches the ground. Since the only necessary analytical modification in a new stochastic process of rainfall reaching the ground is the reduction of the rate of storm arrivals, λ, the rainfall process is transformed into a new stochastic process with a parameter $\lambda' = \lambda e^{-\Delta/\alpha}$ [see *Rodríguez-Iturbe and Porporato*, 2004]. Saturation overland flow is derived from rainfall excess, which occurs when rainfall depth exceeds the available storage.

2.3. Water Loss From the Soil

[10] Leakage losses are assumed to occur through gravitational flow. $L(s)$ is assumed to be at its maximum for saturated soil moisture conditions and can be expressed using the hydraulic conductivity $K(s)$:

$$L(s) = K(s) = \frac{K_{sat}}{e^{\beta(1-s_{fc})} - 1}\left[e^{\beta(s-s_{fc})} - 1\right], \quad \text{for} \quad s_{fc} < s \le 1, \tag{2}$$

where K_{sat} is the saturated hydraulic conductivity, s_{fc} is s at "field capacity," when $K(s)$ has a value of zero, and β is a parameter that can be obtained by fitting the power law unsaturated hydraulic conductivity, $K(s) = K_{sat}\, s^{\beta-1}$, or the soil-water retention curve, $\Psi = \Psi_s\, s^{-\beta/2+2}$, to the field data (where Ψ is the soil matrix potential and Ψ_s is the fitted parameter denoting Ψ at the air entry) [*Clapp and Hornberger*, 1978].

[11] In this model, the main limiting factor controlling the evapotranspiration is considered to be s, giving

$$E(s,t) = \begin{cases} 0, & \text{for} \quad 0 < s \le s_h \\ E_W \dfrac{s - s_h}{s_W - s_h}, & \text{for} \quad s_h < s \le s_W \\ E_W + (E_{\max} - E_W)\dfrac{s - s_W}{s^* - s_W}, & \text{for} \quad s_W < s \le s^* \\ E_{\max}, & \text{for} \quad s^* < s \le 1 \end{cases}, \tag{3}$$

where E_W and $E_{\max}$ are the soil evaporation and the maximum evapotranspiration, respectively, and s_h, s_W and s^* are s at "hygroscopic point," "plant wilting point" and "plant stress point," respectively. The primary forcing variable for evapotranspiration in the tropics is net available energy. Thus, we use a modified *Priestley and Taylor* [1972] expression to compute E_W and $E_{\max}$ given by

$$E_{W \text{ or } \max} = \alpha_{PT\_W \text{ or } \max} \frac{\delta}{L_v \rho_w (\delta + \Gamma)} R_n, \tag{4}$$

where α_{PT_W} and $\alpha_{PT\_\max}$ are the Priestley–Taylor coefficients for E_W and $E_{\max}$, respectively, δ is the rate of change of saturation water vapor pressure with temperature, L_v is the latent heat of vaporization of water, ρ_w is the density of water, Γ is the psychrometric constant, and R_n is the net radiation above the canopy. All thermodynamic variables in equation (4) are assumed to be constant values, and R_n is also obtained by averaging seasonally observed values, to maintain analytical tractability. Note that using averaged R_n,

resulting in an averaged value of evapotranspiration, causes little change to the probabilistic description of soil moisture [*Kumagai et al.*, 2004b].

2.4. Probability Distribution of Soil Moisture

[12] Owing to the stochastic rainfall forcing in equation (1), its solution can be represented only in a probabilistic manner. In this framework, the probability density function (pdf) of s ($pdf(s)$) can be derived from the equation of the process considering the Markov property to give

$$pdf(s) = \begin{cases} \dfrac{C}{\eta_W}\left(\dfrac{s-s_h}{s_W-s_h}\right)^{\frac{\lambda'(s_W-s_h)}{\eta_W}-1} e^{-\gamma s}, & \text{for} \quad s_h < s \le s_W \\ \dfrac{C}{\eta_W}\left[1+\left(\dfrac{\eta}{\eta_W}-1\right)\left(\dfrac{s-s_W}{s^*-s_W}\right)\right]^{\frac{\lambda'(s^*-s_W)}{\eta-\eta_W}-1} e^{-\gamma s}, & \text{for} \quad s_W < s \le s^* \\ \dfrac{C}{\eta} e^{-\gamma s+\frac{\lambda'}{\eta}(s-s^*)}\left(\dfrac{\eta}{\eta_W}\right)^{\lambda'\frac{s^*-s_W}{\eta-\eta_W}}, & \text{for} \quad s^* < s \le s_{fc} \\ \dfrac{C}{\eta} e^{-(\beta+\gamma)s+\beta s_{fc}}\left[\dfrac{\eta e^{\beta s}}{(\eta-m)e^{\beta s_{fc}}+m e^{\beta s}}\right]^{\frac{\lambda'}{\beta(\eta-m)}+1}\left(\dfrac{\eta}{\eta_W}\right)^{\lambda'\frac{s^*-s_W}{\eta-\eta_W}} e^{\frac{\lambda'}{\eta}(s_{fc}-s^*)}, & \text{for} \quad s_{fc} < s \le 1 \end{cases} \tag{5}$$

in which

$$\eta_W = \frac{E_W}{nZ_r}, \tag{6}$$

$$\eta = \frac{E_{\max}}{nZ_r}, \tag{7}$$

$$\gamma = \frac{nZ_r}{\alpha}, \tag{8}$$

$$m = \frac{K_{sat}}{nZ_r\left[e^{\beta(1-s_{fc})}-1\right]}, \tag{9}$$

where C is an integration constant, which can be found by normalizing $pdf(s)$ so that $\int_{s_h}^{1} pdf(s)ds = 1$.

2.5. Representation of Seasonal and Year-to-Year Variations in the Probability Distribution of Soil Moisture

[13] To avoid a nonstationarity issue, we divided the year into wet and dry seasons (described later). Equation (5) describes the steady state $pdf(s)$ over a given season. Therefore, the calculation of equation (5) was applied to find two different pdf's using a separate set of parameters for each season [*Miller et al.*, 2007]. A composite $pdf(s)$ was then created by a simple weighting method proposed by *Miller et al.* [2007]:

$$pdf_{\text{Whole}}(s) = \omega_{\text{Wet}} pdf_{\text{Wet}}(s) + \omega_{\text{Dry}} pdf_{\text{Dry}}(s), \tag{10}$$

where pdf_{Whole} is the composite pdf for a whole year, and pdf_{Wet} and pdf_{Dry} are the individual pdf's for the fractions of the year corresponding to the wet (ω_{Wet}) and dry seasons (ω_{Dry}), respectively.

[14] In addition, the effects of interannual climate fluctuations on pdf_{Whole}, pdf_{Wet} and pdf_{Dry} are incorporated by studying the interannual variability of λ and α for each season. The fluctuations of these parameters are represented by gamma distributions based on their means (μ) and standard deviations (σ), and are obtained from the respective year-to-year variations from the long-term precipitation data at a given site. Therefore, pdf_{Wet} and pdf_{Dry} (and thus $pdf_{\text{Whole}}(s)$) are calculated using equation (5) with the pairs of λ and α generated by Monte Carlo sampling using gamma distributions for the wet and dry seasons [see *D'Odorico et al.*, 2000].

3. Study Sites

[15] In this study, we present an analysis of soil moisture dynamics at a TRF and a TSF site in SEA where vegetation–atmosphere exchange and meteorological data, well suited for estimating the ecohydrological model parameters, are available; there are only a few such tropical forest sites in SEA [see *Tanaka et al.*, 2008]. While details of the study sites and instruments in the TRF and the TSF have been presented in the previous studies by *Komatsu et al.* [2003], *Kumagai et al.* [2004a, 2004b, 2004c, 2005, 2006], *Kume et al.* [2007], and *Tanaka et al.* [2003, 2004], a review synthesizing the descriptions relevant to hydrologic cycles at these two sites is provided for completeness.

[16] The experiments were carried out at two natural evergreen forest sites for TRF and TSF. The TRF and TSF sites are located in Lambir Hills National Park (LHNP; 4°12′N, 114°02′E, 200 m a.s.l.) 30 km south of Miri City, Sarawak, Malaysia, and Kog-Ma Experimental Watershed (KMEW; 18°48′N, 98°54′E, 1265–1420 m asl) adjacent to Chiang Mai, Thailand.

3.1. Tropical Rain Forest Site

[17] In LHNP, a 4 ha experimental plot gridded into 400 subplots or quadrats of 10 m × 10 m was set, and an 80-m-tall (at the base of the gondola) canopy crane with a 75-m-long rotating jib was constructed at the center of this plot to provide access to the upper canopy. Some observational floors of the canopy crane were devoted to eddy-covariance flux measurements and above-canopy meteorological measurements such as radiation flux, air temperature and humidity, wind velocity and rainfall. The subplots or quadrants were used for throughfall and stemflow measurements, in-canopy micrometeorological measurements and soil moisture measurements.

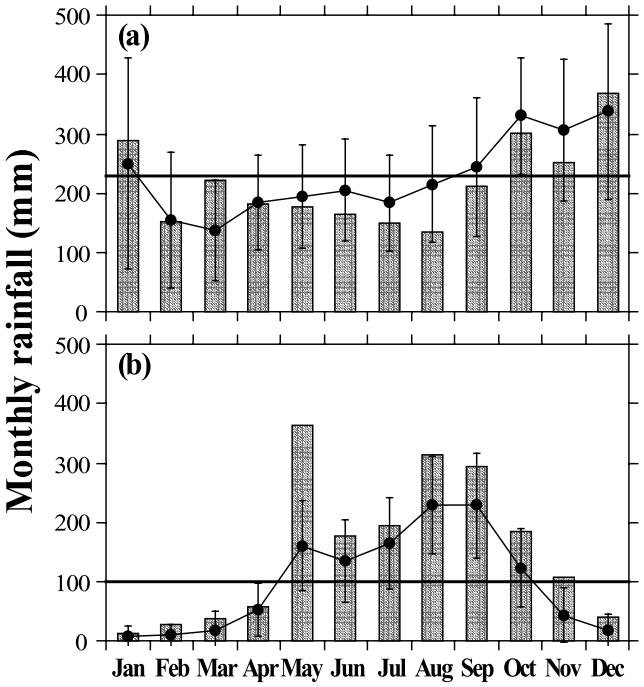

Figure 1. Monthly mean rainfall (columns) at (a) Lambir Hills National Park for the period 2000–2006 and (b) Kog-Ma Experimental Watershed for the period 1998–2002. The points with error bars show the means±standard deviations of the monthly rainfall at Miri Airport for the period 1968–2001 (Figure 1a) and at Chiang Mai Airport for the period 1951–2000 (Figure 1b). The thick horizontal lines are yearly average rainfalls (mm month^{-1}) at these airports divided among months.

[18] The rain forest in LHNP consists of two types of original vegetation common to Borneo, mixed dipterocarp and tropical heath forest. The former contains various genera of the family Dipterocarpaceae, which cover 85% of LHNP. The canopy height surrounding the crane is about 40 m but the height of the emergent treetops can reach 50 m. The leaf area index (LAI) ranged spatially from 4.8 to 6.8 m^2 m^{-2} with a mean of 6.2 m^2 m^{-2}. The monthly amounts of litterfall were similar throughout the year, perhaps suggesting small variations in the LAI. The soils consist of red-yellow podzonic soils (Malaysian classification) or ultisols (U.S. Department of Agriculture Soil Taxonomy), with high sand content (62–72%), accumulation of nutrient content at the surface horizon, low pH (4.0–4.3), and high porosity (54–68%).

[19] The mean annual rainfall at Miri Airport, 20 km from LHNP, for the period 1968–2001 was around 2740 mm, while in LHNP for the period 2000–2006 the value was around 2600 mm (Figure 1a). The long-term record at Miri Airport shows the significant interannual variations in rainfall in this region; for example, the maximum and minimum annual rainfalls for 1968–2001 were 3499 mm in 1988 and 2125 mm in 1976, respectively. Annual rainfall cycles at Miri Airport and in LHNP were similar: the drier and wetter months were between February and September and between October and January, respectively, at both locations (Figure 1a). The mean annual temperature in LHNP is around 27°C with little seasonal variation. Note that in accord with the definition of tropical regions by the International Hydrological Program (IHP) of UNESCO [*Chang and Lau*, 1993], both Miri Airport and LHNP were categorized into "Humid Tropics."

3.2. Tropical Seasonal Forest Site

[20] An 8.63 ha subwatershed of KMEW and a 50 m meteorological tower constructed on the ridge of the subwatershed were used in this study. Eddy-covariance measurements and above-canopy micrometeorological measurements, such as those of radiation flux, air temperature and humidity and wind velocity, were conducted on the tower. Soil moisture adjacent to the tower was also measured. A quadrat near the tower was devoted to throughfall and stemflow measurement. Furthermore, in this subwatershed, streamflow was measured using a weir and rainfall was measured in an open space near the weir, allowing the water budget to be estimated.

[21] Forested areas in northern Thailand are among the most important TSF in SEA in terms of the percent forest cover [*National Park, Wildlife and Plant Conservation Department*, 2000]. Hill evergreen forests, which are one of the typical forest types in northern Thailand [*Tanaka et al.*, 2008], in KMEW are composed exclusively of evergreen trees. The dominant tree family in the subwatershed is Fagaceae. The uppermost story of the canopy in the site ranged 25–40 m and the tallest trees near the tower were 33 m high. The LAI measured near the tower was 4.0 m^2 m^{-2}. The forest floor soils are derived from granitic materials and are classified as reddish brown lateritic soils (Thailand classification) or ustults (U.S. Department of Agriculture Soil Taxonomy) with around 50% sand content and high porosity (60–70%).

[22] The mean annual rainfall at Chiang Mai Airport, 10 km from KMEW, for the period 1951–2000 was around 1190 mm, while that at KMEW for the period 1998–2002 was around 1810 mm (Figure 1b). *Kuraji et al.* [2001] reported that in this region, the higher altitudes have strong tendency to receive higher precipitation. Although KMEW is near Chiang Mai Airport, the airport is located around 310 m asl. Thus, the significant difference in annual rainfall amount between the two locations is probably caused by orographic enhancement of rainfall. Note that unlike the case for the TRF site, there is a distinct seasonal variation in rainfall at the TSF site; in both KMEW and at Chiang Mai Airport, the drier and wetter periods were November–April and May–October, respectively (Figure 1b). The long-term record at the airport also revealed that there is an appreciable interannual variation in rainfall in this region; for example, the maximum and minimum annual rainfalls for 1951–2000 were 1997 mm in 1953 and 739 mm in 1993. The mean annual temperature at the TSF site was around 20°C with a 6°C seasonal range. It should be noted that KMEW and Chiang Mai are classified as "Subhumid Tropics" and "Wet-dry Tropics" using the IHP definition [*Chang and Lau*, 1993] and thus potential vegetation type for both regions is TSF.

4. Data and Model Parameter Estimation

4.1. Soil and Evapotranspiration Parameters

[23] Table 1 gives the model parameters for evapotranspiration and soil characteristics for computing the soil

Table 1. Model Parameters of Evapotranspiration and Soil Characteristic for Lambir Hills National Park and Kog-Ma Experimental Watershed

Variable	Equation	Value	
		LHNP[a]	KMEW[b]
Z_r	(1)	1.0 (m)	5.0 (m)
n	(1)	0.36	0.4
K_{sat}	(2)	33.4 (mm d^{-1})	54.2 (mm d^{-1})
β	(2)	6.3	14.6
s_h	(3)	0.05	0.06
s_W	(3)	0.1	0.06
s^*	(3)	0.34	0.06
s_{fc}	(2) and (3)	0.34	0.47
α_{PT_W}	(4)	0.57	0
α_{PT_max}	(4)	0.82	0.55
R_n for wet season	(4)	128.3 (W m^{-2})	117.4 (W m^{-2})
R_n for dry season	(4)	140.3 (W m^{-2})	113.9 (W m^{-2})
Δ	$\lambda' = \lambda\, e^{-\Delta/\alpha}$ (see text)	1.10 (mm)	0.94 (mm)

[a]Lambir Hills National Park.
[b]Kog-Ma Experimental Watershed.

moisture dynamics in LHNP and KMEW. Here, we present how these parameters were derived and validate the model.

[24] In LHNP, the roots concentrate in a soil depth of less than 0.5 m (T. Kume, personal observation) and the major soil moisture dynamics are mainly the result of root water absorption occurring to a depth of around 1.0 m. On the other hand, in KMEW, a rooting depth of 4.0–5.0 m was assumed to explain the late dry season transpiration peak for the year. This assumption is consistent with the results of a soil penetration test, which showed soil became harder at a depth of 4.0–5.0 m [*Tanaka et al.*, 2004]. Thus, we assumed Z_r to be 1.0 m for LHNP and 5.0 m for KMEW. The parameters, n and s_h, corresponding to the saturated and residual water contents, respectively, for LHNP and KMEW were estimated using the soil water retention curves obtained at the respective sites [*Kumagai et al.*, 2004a, 2004b; *Tanaka et al.*, 2004].

[25] The ultisols at LHNP, which are classified as an argillic soil, have a very high sand content, and therefore acts like sand in terms of water movement at high Ψ, but retains water like clay soils at lower Ψ [*Kumagai et al.*, 2004c]. In fact, K_{sat} and β at this site, which were estimated using nonlinear least squares regression between the time courses of s by a numerical solution of equation (1) and the observations [*Kumagai et al.*, 2004a, 2004b], are typical for sandy clay – silty clay loam and sand, respectively [see *Campbell and Norman*, 1998]. For KMEW, β was estimated using the soil water retention curve [*Tanaka et al.*, 2004] and was categorized as clay loam, and thus K_{sat} at this site was determined as that of clay loam [see *Campbell and Norman*, 1998].

[26] A major uncertainty in equation (4) is α_{PT}, which for forested ecosystems, is usually less than its typical 1.26 value because of an additional boundary layer, leaf, xylem and root resistances. For both sites, we used the eddy covariance measured evapotranspiration to obtain daily α_{PT} and then proceeded to derive the relationships between s and daily α_{PT} [see *Kumagai et al.*, 2004b]. As a result, the $s - \alpha_{PT}$ relationships provided the values of α_{PT_W} and α_{PT_max} in LHNP [*Kumagai et al.*, 2004a, 2004b] and KMEW (N. Yoshifuji, unpublished data, 2009).

[27] s_{fc} was assumed to be s at each site when L(s) in χ in equation (1) (=$L(s) + E(s, t)$) cannot be ignored and thus $L(s) = K(s) = 0.1$ mm d^{-1}. The values of s_h and s_W for LHNP were estimated using the $s - \alpha_{PT}$ relationship [*Kumagai et al.*, 2004a, 2004b]. Since there was no evapotranspiration plateau at high s at this site, s^* was assumed to be equal to s_{fc}. In KMEW, although the s range observed was limited, α_{PT} was constant regardless of s (N. Yoshifuji, unpublished data, 2009). Hence we assumed $s_h = s_W = s^*$; i.e., α_{PT} abruptly decreases to zero at s_h and has a constant value for E_{max} throughout the $s > s_h$ range.

[28] For both sites, the mean daily R_n values in the wet and dry seasons were obtained; in LHNP, R_n in the wet season is lower than that in the dry season owing to cloud cover effects, but in KMEW, a decrease in R_n caused by cloud cover in the wet season was compensated for by the maximal solar elevation during the wet season, and thus values for R_n in the wet and dry seasons are similar in value.

[29] Throughfall and stemflow only occur when rainfall exceeds certain thresholds and can be described as linear functions of rainfall. Consequently, the daily interception loss was related to incident rainfall in a single storm event by subtracting both the throughfall and stemflow functions from rainfall in LHNP [*Manfroi et al.*, 2006] and KMEW (N. Tanaka, unpublished data, 2009). Thus, for both sites, Δ, the amount of rainfall that can accumulate on forest canopy during a rainfall event, was calculated from the daily interception functions of rainfall.

[30] Using the above model parameters and time courses of rainfall as local forcing data, the soil moisture balance

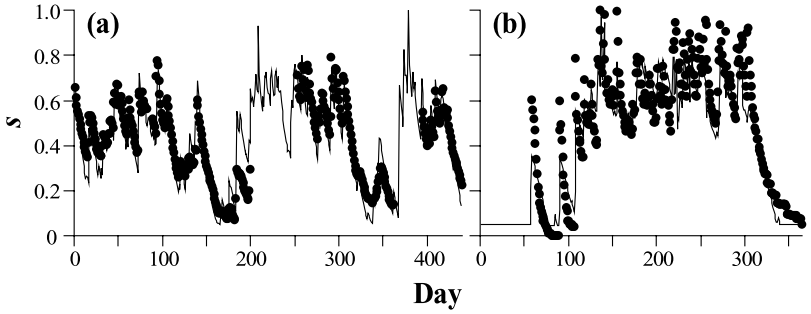

Figure 2. Time series of measured (solid circles) and calculated (curves) daily average soil moisture content (s) in (a) Lambir Hills National Park and (b) Kog-Ma Experimental Watershed. The measurement period for Figure 2a was day of year (DOY) 78, 2001 to DOY 151, 2002 and for Figure 2b was DOY 1 to DOY 366, 2000.

Table 2. Mean Yearly Rainfall Parameters (±Standard Deviation) for Wet and Dry Seasons in Miri and Chiang Mai[a]

	Miri		Chiang Mai	
Parameter	Wet[b]	Dry[c]	Wet[d]	Dry[e]
P[f] (mm)	1470.7 ± 378.3	1273.0 ± 218.8	1039.3 ± 203.8	149.0 ± 73.0
λ (d^{-1})	0.63 ± 0.079	0.46 ± 0.057	0.55 ± 0.049	0.093 ± 0.027
α (mm)	15.1 ± 2.84	12.9 ± 1.63	10.2 ± 1.66	8.60 ± 3.40

[a]Values in Miri and Chiang Mai were the averages over the studied periods 1968–2001 and 1951–2000, respectively.
[b]September–January (153 days).
[c]February–August (212 days).
[d]May–October (184 days).
[e]November–April (181 days).
[f]Rainfall amount.

model was validated in a deterministic mode (i.e., not using probabilistic descriptions) for each study site (Figure 2). Note that the soil domain of measured and modeled s was 0–0.5 m depth for both LHNP and KMEW. The model well reproduces the canonical structure of s time series measurements for both study sites despite all the simplifying assumptions. Especially, the validity of the model having the assumptions that leakage loss occurs only through gravitational flow, as described in equation (2), and that lateral flow can be neglected, suggests that the soil moisture dynamics model in this study, which was originally developed for applications in flat semiarid areas [see *Rodríguez-Iturbe and Porporato*, 2004], can be applied to the humid and somewhat nonflat environments of this study's sites.

4.2. Precipitation Characteristics

[31] We discuss first the precipitation characteristics at TRF and TSF sites using the long-term records obtained at the Miri and Chiang Mai airports, respectively, and then proceed to discuss their usage for constructing rainfall parameters in the model examining the soil moisture dynamics in LHNP and KMEW.

[32] Especially at the TSF site, a clear distinction between wet and dry seasons exists in the annual rainfall cycle. Therefore, we divided the year into two periods using the value of yearly average rainfall divided by months; the periods when the monthly mean rainfalls were above and below the value were classified as wet and dry seasons, respectively (Figure 1). As a result, the periods for wet and dry seasons were September–January (153 days) and February–August (212 days) for the TRF site and May–October (184 days) and November–April (181 days) for the TSF site (see Table 2).

[33] Figures 3 and 4 show the time series of yearly precipitation (P), λ and α for the wet and dry seasons at the TRF and TSF sites, respectively. Figures 3 and 4 also show how P, λ and α for each season responded to ENSO and the long-term trends in these rainfall parameters, for each site. In Miri, despite the dry season being 60 days longer than the wet season, the mean yearly P in the wet season was around 200 mm higher than that in the dry season (Table 2). In addition, the mean yearly λ and α in the wet season were significantly higher than those in the dry season. On the other hand, in Chiang Mai, all parameters P, λ and α were considerably higher in the wet season than in

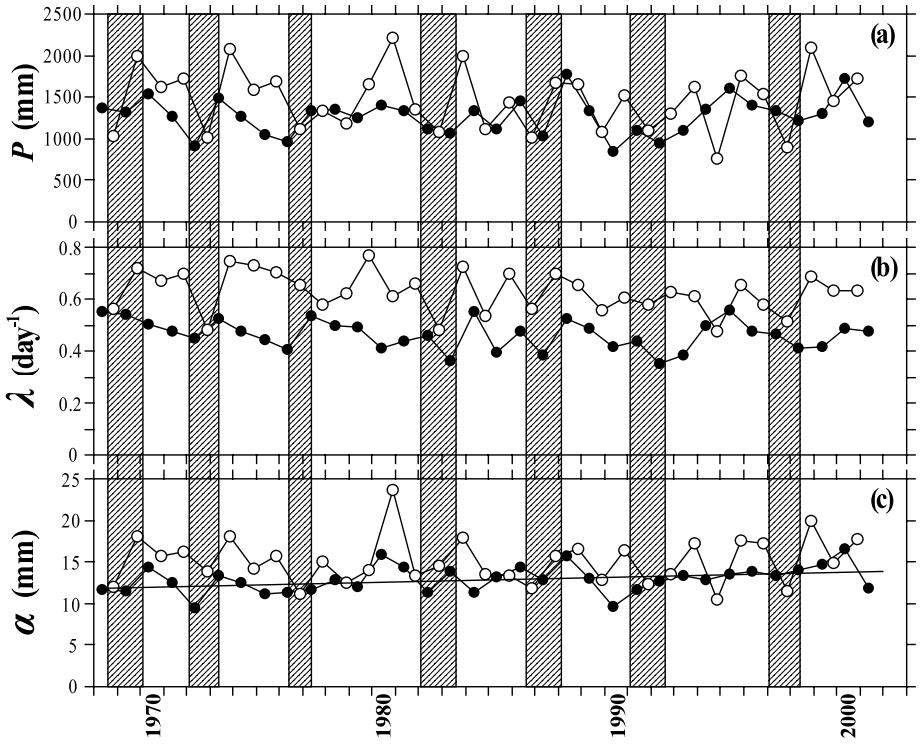

Figure 3. Time series of (a) total seasonal rainfall (P), (b) the estimated seasonal rate of arrival of storms (λ), and (c) the seasonal average storm depth (α) based on daily data of precipitation at Miri. Open and closed circles denote wet and dry seasons, respectively. Shaded columns represent the periods of El Niño events, and the regression line is shown where significant ($p < 0.05$).

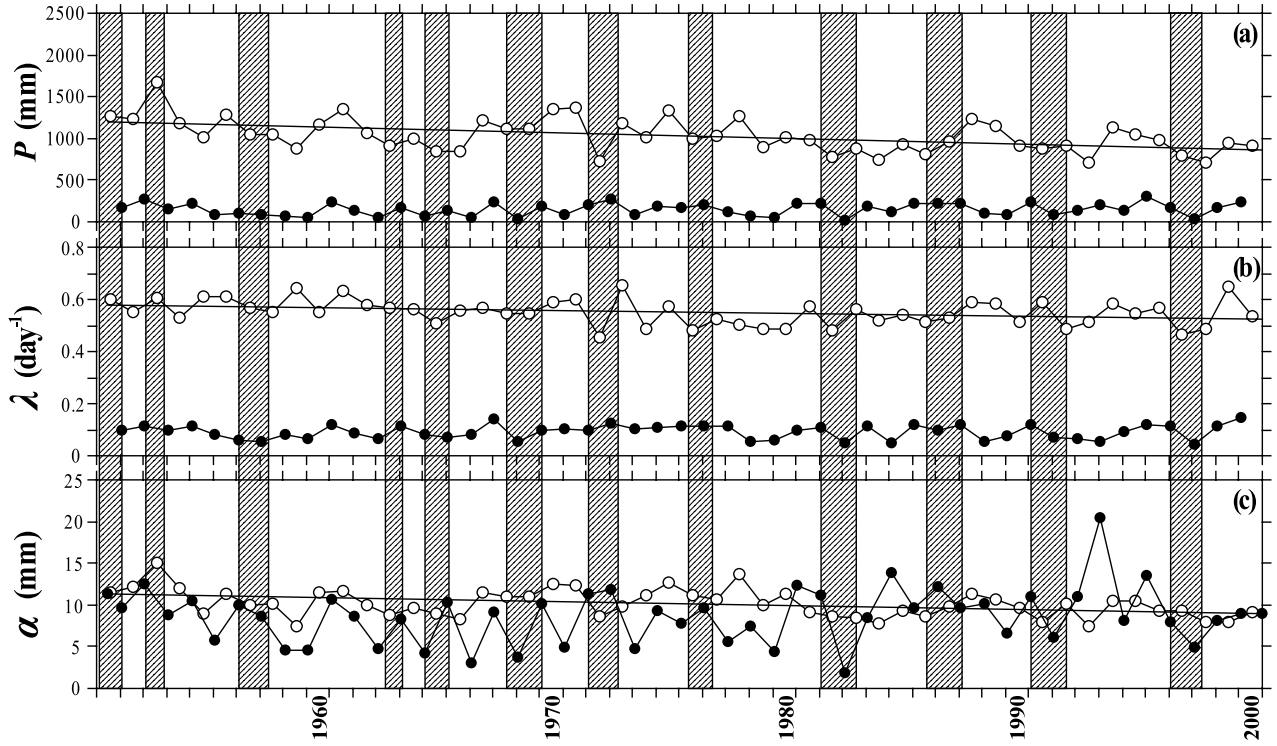

Figure 4. Same as Figure 3 but at Chiang Mai.

the dry season (Table 2). It should be noted that the mean yearly P per day and α in the dry season in Miri were significantly higher than those in the wet season in Chiang Mai, suggesting that the TSF site, Chiang Mai, is drier, even in the wet season, than the TRF site, Miri.

[34] In Miri, only yearly α in the dry season had a clear long-term trend with statistical significance ($p < 0.05$), and it showed a rising tendency (Figure 3). In Chiang Mai, all rainfall parameters, yearly P, λ and α, in the wet season significantly decreased ($p < 0.05$) (Figure 4). Mean yearly P, λ and α in both seasons in Miri and Chiang Mai under El Niño and normal conditions are given in Table 3 (also see Figures 3 and 4). There were no significant differences in the parameters in the dry season for Miri and both seasons for Chiang Mai (except for λ in the wet season for Chiang Mai). However, all parameters under an El Niño condition were significantly different from those under a normal condition in the wet season for Miri (Cochran–Cox test (two independent sample means t test without homogeneity of variance), $p < 0.05$), suggesting that Miri was drier in ENSO events only in the wet season and that this decrease in rainfall amount was caused by the reductions in both the rate of arrival of storms and the storm depth.

[35] *Malhi and Wright* [2004] also reported that ENSO is the primary driver of precipitation fluctuations for large areas of SEA, but that over a long-term period, precipitation appears to have declined marginally in the TRF regions. At the TRF site, Miri, however, although the reduction in the rainfall amount and the controlling parameters (i.e., λ and α) occurred in the wet season under an ENSO condition, we found no or weak long-term trends in the rainfall parameters. *Zhang et al.* [2002] also found that ENSO is related to a reduction in annual precipitation on the Indochina Peninsula. We found that at the TSF site, Chiang Mai, declining long-term tendencies in the rainfall amount and the controlling parameters exist only in the wet season, but that the El Niño effect in reducing rainfall is weak. This inconsistency might have resulted partly from our TSF site being located in an inland area of Thailand.

[36] Correlation characteristics between λ and α and between these two parameters and P in the wet and dry seasons for Miri and Chiang Mai are given in Table 4. As expected, the yearly seasonal P is highly correlated with the values of λ and α in the same year but not for the dry season at Miri; it is interesting to note that only in the dry season for Miri could neither λ nor α explain the seasonal P in the same year. The correlations between λ and α in all cases

Table 3. Mean Yearly Rainfall Parameters (±Standard Deviation) for El Niño and Normal Conditions

Data	Parameter[a]	El Niño Conditions	Normal Conditions
Miri_wet	P[b] (mm)	1217.4 ± 367.7	1565.7 ± 342.9
	λ[b] (d^{-1})	0.58 ± 0.088	0.65 ± 0.070
	α[b] (mm)	13.5 ± 2.34	15.8 ± 2.79
Miri_dry	P (mm)	1263.4 ± 203.1	1277.6 ± 230.1
	λ (d^{-1})	0.45 ± 0.068	0.47 ± 0.051
	α* (mm)	12.4 ± 1.36	13.2 ± 1.71
Chiang Mai_wet	P* (mm)	985.5 ± 246.0	1060.2 ± 184.5
	λ*[b] (d^{-1})	0.53 ± 0.052	0.56 ± 0.047
	α* (mm)	9.96 ± 1.82	10.3 ± 1.61
Chiang Mai_dry	P (mm)	140.8 ± 81.6	152.0 ± 70.7
	λ (d^{-1})	0.087 ± 0.030	0.096 ± 0.026
	α (mm)	8.23 ± 3.17	8.74 ± 3.51

[a]Asterisks denote data detrended using linear regression lines (see Figures 2 and 3).
[b]Significant differences according to the Cochran–Cox test (two independent sample means t test without homogeneity of variance) ($p < 0.05$).

Table 4. Correlations Characteristic of the Rainfall Regime in the Same Year for Wet and Dry Seasons in Miri and Chiang Mai

Data	Correlations	R^2	p
Miri_wet	$\alpha-\lambda$[a]	0.17	0.016
	$\lambda-P$[b]	0.57	<0.0001
	$\alpha-P$[c]	0.82	<0.0001
Miri_dry	$\alpha-\lambda$	0.0025	0.78
	$\lambda-P$	0.0083	0.61
	$\alpha-P$	0.018	0.45
Chiang Mai_wet	$\alpha-\lambda$	0.013	0.43
	$\lambda-P$	0.29	<0.0001
	$\alpha-P$	0.81	<0.0001
Chiang Mai_dry	$\alpha-\lambda$	0.050	0.12
	$\lambda-P$	0.59	<0.0001
	$\alpha-P$	0.58	<0.0001

[a]Correlation of the rate of arrival of storms (λ) and the average storm depth (α).
[b]Correlation of total seasonal rain (P) and λ.
[c]Correlation of P and α.

were very weak or nonexistent (Table 4), and thus the parameters can be modeled as independent of each other. Furthermore, at both locations, none of the rainfall parameters (P, λ, α) exhibited significant temporal (season-to-season) autocorrelation (for example, α in the 1987 wet season was not correlated with α in the 1988 dry season in Miri), permitting us to independently determine each rainfall parameter in wet and dry seasons and compute a whole-year pdf for s using the simple weighting method, equation (10) (data not shown).

[37] Mean yearly P in LHNP in wet and dry seasons for the period 2000–2006 were 1422.3 and 1178.5 mm, respectively, and the ratios to the respective seasonal rainfall in Miri were 0.97 and 0.93 (see Figure 1 and Table 2). Thus, we assumed that we can use the rainfall parameters in Miri for calculating the soil moisture dynamics in LHNP. The mean yearly P in KMEW for the period 1998–2002 was appreciably larger than that in Chiang Mai; the mean yearly P in KMEW and the ratios to those in Chiang Mai for the wet and dry seasons were 1526.0 and 281.2 mm and 1.47 and 1.89, respectively (see Figure 1 and Table 2). In this region, *Kuraji et al.* [2001] found that rainfall amount increases with altitude and that this increase is due to the increase in rainfall duration, not rainfall intensity. This implies the larger rainfall amount in KMEW can be reproduced by multiplying λ by the factors 1.47 for the wet season and 1.89 for the dry season and retaining α for Chiang Mai because the mean rainfall for a given period is $D \times \lambda \times \alpha$ (where D is the number of days in a given period). Note that since both KMEW and Chiang Mai are typical of TSF, the KMEW rainfall characteristics derived from that of Chiang Mai using the above reasonable procedure are valid for general examinations of ecohydrological processes in TSF in SEA.

[38] Figure 5 compares the histograms of relative frequencies of λ and α between Miri and Chiang Mai and between wet and dry seasons. In Miri, the frequency distributions of both λ and α in the wet and dry seasons overlap at their tails (Figures 5a and 5c), while differences in λ and α between wet and dry seasons were significant ($p < 0.0001$ and $p = 0.00014$, respectively). However, in Chiang Mai, while the distribution of α in the wet and dry seasons overlap at the tails, those of λ barely overlap (Figures 5b and 5d). Also here, the differences in λ and α between wet and dry seasons were significant ($p < 0.0001$ and $p = 0.0024$, respectively). Two parameter (μ and σ) gamma distributions were fitted to the histograms, and year-to-year variations in λ and α were described using random numbers generated from the probability distributions. Again, note that both μ and σ for the λ histograms in Chiang Mai were multiplied by the factors 1.47 for the wet

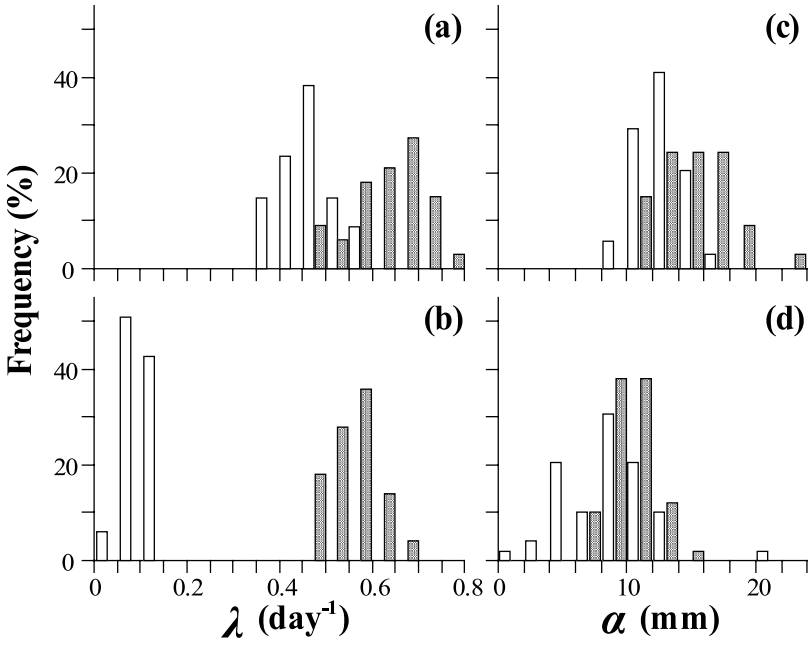

Figure 5. Frequency distribution of the seasonal rate of arrival of storms (λ) and the seasonal average storm depth (α) based on daily data of precipitation at (a and c) Miri and (b and d) Chiang Mai. Blank and shaded columns represent the frequencies in the dry and the wet seasons, respectively.

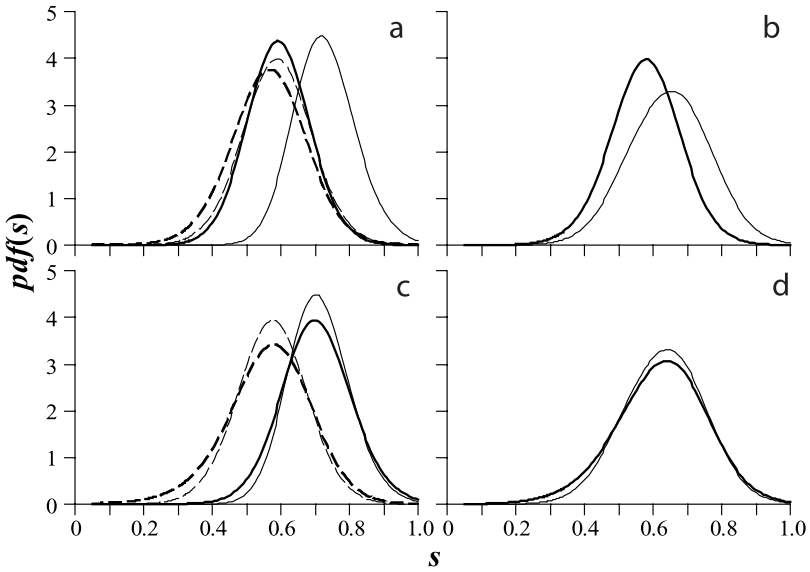

Figure 6. Probability density function of relative soil moisture (*pdf*(*s*)) in Lambir Hills National Park using rainfall parameters λ and α under the El Niño conditions of 1997–1998 (Figures 6a and 6b) and generated from the gamma distributions in Figure 5, which take into consideration the year-to-year variations in rainfall (Figures 6c and 6d). Thick solid and broken curves denote the wet and dry seasons, respectively (Figures 6a and 6c), and thick solid curves denote the whole year (Figures 6b and 6d). As a reference, the corresponding probability density function lines calculated using the rainfall parameters averaged throughout the study period are also represented (thin curves).

season and 1.89 for the dry season to obtain λ for computing soil moisture dynamics in KMEW.

5. Model Results and Discussion

[39] The TRF and TSF sites, i.e., Miri and Chiang Mai, apparently differ in terms of the rainfall amount in wet and dry seasons. Further analyses of rainfall parameters λ and α revealed that while there was no or weak long-term trend in rainfall amount and characteristics at the TRF site, the TSF site had a long-term decrease in the rainfall in the wet season, and that ENSO reduced the rainfall amount and characteristics only in the wet season at the TRF site. Thus, considering these remarkable rainfall contrasts between the TRF and TSF sites, we now examine the soil moisture dynamics at the TRF and TSF sites, i.e., LHNP and KMEW, using stochastic representations.

5.1. Lambir Hills National Park

[40] In LHNP, severe drought associated with the ENSO event of 1997–1998 induced higher tree mortality, implying its significant impact on forest ecosystem dynamics [*Nakagawa et al.*, 2000]. Furthermore, results from a global climate model showed more frequent El Niño-like conditions due to human-induced greenhouse warming [*Timmermann et al.*, 1999]. Therefore, it is interesting to compare *pdf*(*s*) under the El Niño condition of 1997–1998, which was extremely strong during the study period [*Nakagawa et al.*, 2000], and under an average condition throughout the study period (Figures 6a and 6b). In the dry season, ENSO has little effect on soil moisture but in the wet season appreciably shifts the *s* distribution to a dry mode, suggesting that the soil moisture dynamics, which might be improbable under average rainfall conditions, can occur in this case (Figure 6a). As a result, on annual timescales, ENSO increases the frequency of *s* in the lower *s* tail (Figure 6b).

[41] Here, we compare *pdf*(*s*) calculated using rainfall parameters λ and α generated from the gamma distributions in Figure 5 that take into consideration the year-to-year variation in rainfall and the rainfall parameters averaged throughout the study period (Figures 6c and 6d). It should be noted that year-to-year variations in rainfall amount and characteristics, in part, are attributed to the drought accompanied by ENSO. The year-to-year variations primarily impact the lower *s* tail of both the seasonal and annual pdf's and have the least impact on the wet mode of *s* (Figures 6c and 6d). In short, interannual fluctuation of precipitation at this site plays a role only in increasing the frequency of the dry mode of *s*. We assumed that this is mainly because at this site, the soil water rapidly drains when the rainwater reaches the ground and is held in the soils with high tension. Thus, we further investigated the effect of the soil texture on *pdf*(*s*) (Figure 7). When changing K_{sat} to that of sandy soil and retaining β, i.e., assuming perfect sandy soil, most rainwater leaks from the soils promptly after rainfall and a small portion of the water is held (Figures 7a and 7b). In contrast, when changing β to that of sandy clay – silty clay loam and retaining K_{sat}, all of pdf_{Wet}, pdf_{Dry} and pdf_{Whole} concentrate in the wet mode (Figures 7c and 7d). Note that in this case the possibility of ponding arises. Figure 7 further suggests that the soil properties, i.e., properties of ultisols in LHNP, are such that a pdf for the whole year is nearly normally distributed with an average of around 0.65 and small tails in the wet and dry modes.

5.2. Kog-Ma Experimental Watershed

[42] Previous studies [*Tanaka et al.*, 2003, 2004] reported that although there is a distinct dry season in KMEW,

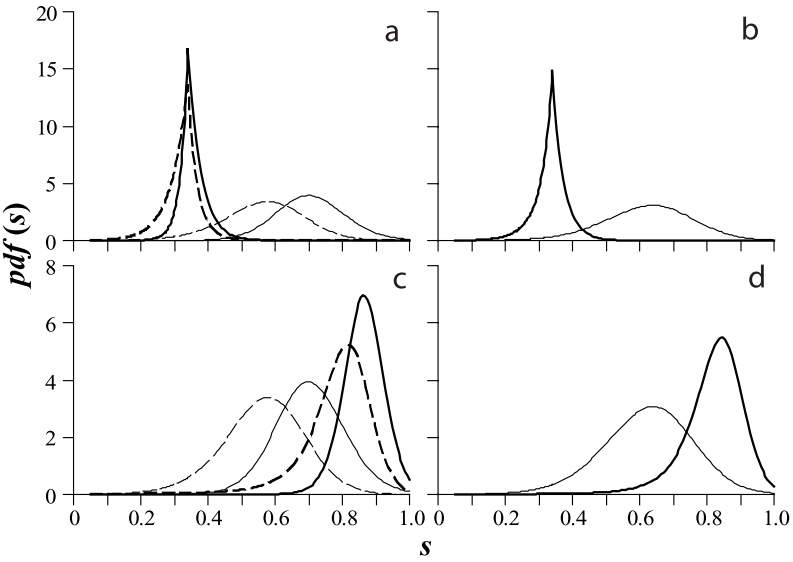

Figure 7. Probability density function of relative soil moisture (*pdf*(*s*)) in Lambir Hills National Park changing K_{sat} to that of sandy soil and retaining β (Figures 7a and 7b) and changing β to that of sandy clay and silty clay loam and retaining K_{sat} (Figures 7c and 7d) (see equation (2)). Thick solid and broken curves denote the wet and dry seasons, respectively (Figures 7a and 7c), and thick solid curves denote the whole year (Figures 7b and 7d). For reference, the corresponding probability density function lines calculated using the original soil property parameters (see Table 1) are also represented (thin curves). Note that all calculations consider the year-to-year rainfall variations.

evapotranspiration from the forest did not decline and furthermore, peaked in the late dry season because of higher evaporative demands in this period. However, we computed pdf_{Dry} using the parameters describing stable evapotranspiration, uncontrolled by s (see Table 1), and found an extremely high probability of the complete depletion of soil water (at s_h) (data not shown). Furthermore, a computation result of the water balance model (equation (1)) in a deterministic mode (Figure 2b) and soil moisture observations at 0–0.5 m showed the complete depletion of soil water at this soil depth and the cessation of evapotranspiration in the dry season. These results are contrary to the fact that even in the dry season, the streamflow was never interrupted and a high evapotranspiration rate was maintained [*Tanaka et al.*, 2003]. Thus, we expect that plant-available soil water was extracted from the deep (blow 5 m depth) forest soil [e.g., *Nepstad et al.*, 1994; *Tanaka et al.*, 2004; *Fisher et al.*, 2007] or the deeper groundwater [e.g., *O'Grady et al.*, 1999; *Čermák and Prax*, 2001; *Vincke and Thiry*, 2008]. Since in KMEW, the mean yearly dry season rainfall amount (~280 mm) was less than the mean yearly dry season evapotranspiration (~310 mm) (data not shown), it is logical to assume that deficit in the forest water use in the dry season is compensated with leakage to the deeper soil or groundwater aquifer in the wet season. Here, we compute pdf_{Dry} assuming evapotranspiration uses soil water derived from a percentage of the average leakage loss $\langle L \rangle$ in the wet season given by [*Rodríguez-Iturbe and Porporato*, 2004]

$$\langle L \rangle = \alpha \left[\lambda' - \lambda' PC(s_{fc}) - \left(\eta + \frac{K_{sat}}{nZ_r} \right) pdf(1) + \eta pdf(s_{fc}) \right] - E_{\max}\left[1 - PC(s_{fc})\right], \quad (11)$$

where $PC(s)$ is the cumulative probability distribution of s. Consequently, we found that to eliminate the high frequency of occurrence of $s = s_h$, 7% of $\langle L \rangle$ in the wet season needs to be used in the evapotranspiration (Figure 8a).

[43] Furthermore, *Tanaka et al.* [2004] claimed that the peak of evapotranspiration at the end of the dry season could be explained by the deep rooting depth (4–5 m) and soil hydraulic properties of silty loam (in their paper, referred to as silty sand according to *Kondo and Xu* [1997]). Thus, on the premise that 7% of $\langle L \rangle$ in the wet season compensates the forest water use deficit in the dry season (see Figure 8a), we examine how varying rooting depth and soil texture impact pdf_{Dry} (Figures 8b and 8c). The computation results for rooting depths of 1–3 m presented an extremely high probability for s_h, whereas for a rooting depth of 5 m there was no tail of the pdf in the dry mode (Figure 8b); these results strongly support the findings of *Tanaka et al.* [2004]. Given the rooting depth of 5 m, changing either or both of K_{sat} or β to the corresponding values for sandy soil moved *pdf*(*s*) to the dry mode and concentrated the distribution to the average value, but there was only small probability for the complete depletion of soil water (Figure 8c). In summary, at this site, rooting depth changed *pdf*(*s*) more drastically than soil texture did, and the deeper ones maintained a stable evapotranspiration rate and moist soil conditions even in the dry season.

[44] It should be noted that Figures 8a, 8b, and 8c show the calculation results using the mean yearly rainfall parameters during the study period. In Figure 8d, we compute *pdf*(*s*) as in Figure 8a, but with a varying supply of water to the forest in the dry season, i.e., considering year-to-year variations in the rainfall parameters. In this case, the higher probability in the dry mode does not disappear, even

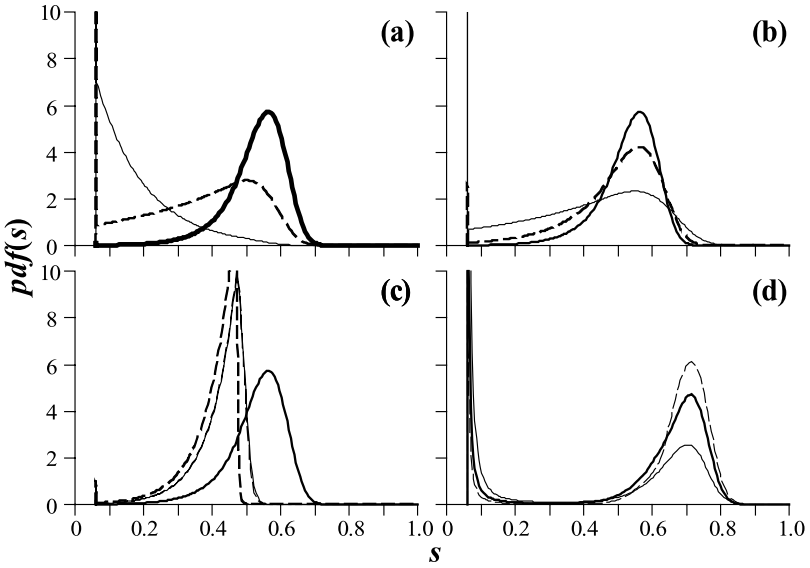

Figure 8. Probability density function of relative soil moisture (*pdf*(*s*)) in Kog-Ma Experimental Watershed in the dry season, when evapotranspiration uses the soil water from 5% (thin solid curve), 6% (thick broken curve), and 7% (thick solid curve) of the average leakage loss in the wet season (Figure 8a); simulated with rooting depths of 1 m (thin solid curve), 3 m (thick broken curve) and 5 m (thick solid curve) (Figure 8b); and retaining both K_{sat} and β of clay loam (thick solid curve), changing only K_{sat} to that of sandy soil (thin broken curve), changing only β to that of sandy soil (thin solid curve) and changing both to those of sandy soil (thick broken curve) (Figure 8c). Figure 8d is the same as Figure 8a but all calculations consider the year-to-year rainfall variations, and here the evapotranspiration uses the soil water from 7% (thin solid curve), 15% (thick solid curve), and 19% (thin broken curve) of the average leakage loss in the wet season. Note that calculations in Figures 8a, 8b, and 8c use average rainfall parameters.

assuming 19% (above which the computation fails as a result of the imbalance of the calculated soil water content) leakage loss in the wet season for the forest water use deficit. This implies that on longer timescales, the forest ecosystem in KMEW can become parched in the dry season, even though it is sufficiently supplied from the water resource in the preceding wet season. Figure 9 further compares the effects of year-to-year variations in rainfall parameters and the average rainfall parameters throughout study period for pdf_{Wet}, pdf_{Dry} and pdf_{Whole} under the "7% water-supply" condition. The canonical structures of both pdf_{Whole} values were bimodal distributions reflecting an apparent difference in rainfall between wet and dry seasons, but *pdf*(*s*) considering the year-to-year rainfall variation had two extremely high probabilities of *s* around complete depletion in the soil water and in the highly wet mode (Figures 9a and 9b).

[45] At this site, to some extent a drought trend during the study period was detected (see Figure 4) and so it is interesting to note how this trend impacts *pdf*(*s*). Here, the study period was divided into three parts, 1951–1967, 1968–1983, and 1984–2000, and we compared *pdf*(*s*) computed using the average rainfall parameters during the period 1951–1967 (wet season: λ = 0.58, α = 10.5; dry

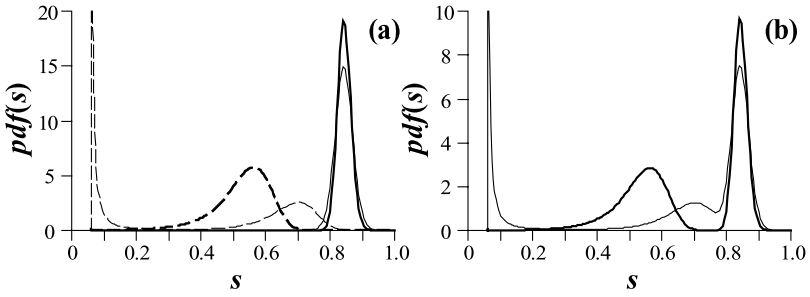

Figure 9. Probability density function of relative soil moisture (*pdf*(*s*)) in Kog-Ma Experimental Watershed considering year-to-year variations in rainfall parameters λ and α in the wet and dry seasons (thin solid and thin broken curves, respectively) and using the rainfall parameters averaged throughout study period in the wet and dry seasons (thick solid and thick broken curves, respectively) (Figure 9a) and in the whole year considering the year-to-year variations (thin solid curve) and using the average parameters (thick solid curve) (Figure 9b). Note that the evapotranspiration uses the soil water from 7% of the average leakage loss in the wet season.

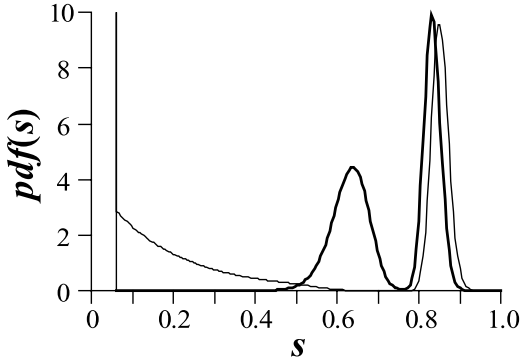

Figure 10. Probability density function of relative soil moisture (*pdf*(*s*)) in Kog-Ma Experimental Watershed in the whole year, using the average rainfall parameters of 1951–1967 (thin solid curve) and 1984–2000 (thick solid curve). Note that the evapotranspiration uses the soil water from 7% of the average leakage loss in the wet season for each study period.

season: $\lambda = 0.091$, $\alpha = 7.90$) and 1984–2000 (wet season: $\lambda = 0.54$, $\alpha = 9.25$; dry season: $\lambda = 0.092$, $\alpha = 10.2$) (Figure 10). The computations suggested a more severe dry soil moisture condition for 1951–1967 than for 1984–2000; in the course of time, pdf_{Wet} slightly moved to a dry mode, whereas pdf_{Dry}, most of which had concentrated at s_h, was near normally distributed and significantly moved to the wet mode (Figure 10). Although there was a drought trend (both rainfall parameters declined with time) in the wet season, both rainfall parameters in the dry season were higher for 1984–2000 than for 1951–1967, and it is not surprising that the soil moisture condition for the whole year became wetter for 1984–2000 than for 1951–2000. This also implies that despite the slight changes in rainfall amount, *pdf*(*s*) appears to be more sensitive to shifts in precipitation in the dry season than in the wet season.

6. Conclusion and Applications

[46] We examined the soil moisture dynamics at a TRF site and TSF site, between which there is a clear difference in the precipitation regime, using a probabilistic ecohydrological model [see *Rodríguez-Iturbe and Porporato*, 2004]. This study primarily set out to elucidate and explain how taking into consideration both seasonal and year-to-year variations in precipitation is crucial for understanding the rainfall–soil moisture behavior in the studied forest ecosystems, LHNP and KMEW, as the TRF and TSF sites, respectively. Thus, first we analyzed interannual fluctuations in precipitation in the studied sites and what the factors were that control them; that is, ENSO-related or not.

[47] Here, we should note that a near normally distributed *pdf*(*s*), i.e., not concentrated in the wet or dry mode, is thought to imply a studied ecosystem's robustness mainly in terms of plant water availability. In LHNP, year-to-year variation increases the frequency of the dry mode of *s* and least impacts the wet mode of *s*; we then assumed that this is mainly attributable to the soil moisture characteristics of the ultisols at LHNP, which acts like sand in terms of water movement and retains water like clay soils. As a result, we concluded that the soil texture in this site contributes to the normal distribution-like *pdf*(*s*) for the whole year with small tails in the wet and dry modes.

[48] However, in KMEW, before considering the effect of year-to-year variations, we could not compute pdf_{Dry} to be consistent with the facts reported in previous studies [*Tanaka et al.*, 2003, 2004] that even in the dry season, the streamflow was never interrupted and a high evapotranspiration rate was maintained. Thus, to obtain a "balanced pdf" for soil moisture, we had to assume that evapotranspiration uses soil water derived from a percentage of the leakage loss in the preceding wet season. Furthermore, we found that a deeper rooting depth maintained stable evapotranspiration even in the dry season. However, we also found that considering year-to-year fluctuations in rainfall, this ecosystem cannot escape from the danger of the depletion of soil water.

[49] Again, year-to-year rainfall variation at the TRF site increases the probability of dry mode occurrence but has little overall effect for the wet mode. Describing the year-to-year variation is necessary for assessing the intensity of severe drought induced by ENSO, leading to high tree mortality [*Nakagawa et al.*, 2000]. Evidence supporting hydraulic constraints within the SPAC as a limit for different plant species to cope with water stress is increasing [e.g., *Pockman and Sperry*, 2000; *Martínez-Vilalta and Piñol*, 2002]. Although several factors establish the capacity of plants to satisfy water demands with the available resources, evaluating the vulnerability to xylem embolism through a SPAC concept is a promising tool for understanding the xylem dysfunction process resulting in plant death [see *Sperry*, 2000; *Sperry et al.*, 2002; *Tyree and Zimmermann*, 2002]. Hence, relating a SPAC model that can predict drought-induced mortality [*Martínez-Vilalta et al.*, 2002] to the stochastic representation of soil moisture dynamics presented in this study could contribute to elucidating the effect of El Niño drought associated with year-to-year rainfall variation and the effect of global climate change on the dynamics of tropical forest ecosystems.

[50] In addition, especially in the studied regions, the stochastic approach describing the soil moisture dynamics under the condition that there are strong perturbations in precipitation is timely because the external hydroclimatic forcing inherently has intermittency in its variability [see *Katul et al.*, 2007]. For example, impacts of terrain disturbance on rainfall–river flow and rainfall–suspended sediment flux responses and soil erosion are among main concerns in terms of the ecological sustainability in TRF areas [e.g., *Chappell et al.*, 1999; *Douglas et al.*, 1999; *Chappell et al.*, 2006]. As *Douglas et al.* [1999] pointed out, these phenomena are episodic, and so the stochastic treatment of rainfall could serve as a tool to provide strategies for soil conservation as a basis for soil–plant system conservation. Moreover, this stochastic analysis could allow the tracking of the relationship between hydroclimatic variability and impacts of shifts in land use on the biosphere–atmosphere exchange in TSF areas [e.g., *Giambelluca et al.*, 1999, 2003], and requires further study.

[51] **Acknowledgments.** We thank Tomoaki Ichie (Kochi University) for providing a long-term rainfall data record obtained at Miri Airport. The rainfall data record at Chiang Mai was obtained by Thai Meteorological Department (TMD) and was provided through the Global Energy and Water Cycle Experiment (GEWEX) Asian Monsoon Experiment (GAME). We

would also like to acknowledge Jun Matsumoto (Tokyo Metropolitan University) for his help in this rainfall data acquisition. This study was supported by the Core Research for Evolutional Science and Technology (CREST) program of the Japan Science and Technology Agency (JST) and Grants-in-Aid for Scientific Research (19255006 and 20380090) from the Ministry of Education, Science and Culture, Japan. We are grateful to Lucy Chong (Forest Research Center, Sarawak Forest Corporation), Tohru Nakashizuka (Tohoku University), and Nipon Tangtham (Kasetsart University) for providing the opportunity of conducting this study and the many colleagues who helped us with field work.

References

Borgogno, E., P. D'Odorico, F. Laio, and L. Ridolfi (2007), Effect of rainfall interannual variability on the stability and resilience of dryland plant ecosystems, *Water Resour. Res.*, *43*, W06411, doi:10.1029/2006WR005314.

Campbell, G. S., and J. M. Norman (1998), *An Introduction to Environmental Biophysics*, 2nd ed., Springer, New York.

Čermák, J., and A. Práx (2001), Water balance of a Southern Moravian floodplain forest under natural and modified soil water regimes and its ecological consequences, *Ann. For. Sci.*, *58*, 63–88.

Chang, J. H., and L. S. Lau (1993), Definition of the humid tropics, in *Hydrology and Water Management in the Humid Tropics*, edited by M. Bonell et al., pp. 571–574, United Nations Educ. Sci., and Cult. Organ.–Cambridge Univ. Press, Cambridge, U. K.

Chappell, N. A., P. McKenna, K. Bidin, I. Douglas, and R. P. D. Walsh (1999), Parsimonious modelling of water and suspended sediment flux from nested catchments affected by selective tropical forestry, *Philos. Trans. R. Soc. London, Ser. B*, *354*, 1831–1846, doi:10.1098/rstb.1999.0525.

Chappell, N. A., K. Bidin, and W. Tych (2001), Modelling rainfall and canopy controls on net-precipitation beneath selectively logged tropical forest, *Plant Ecol.*, *153*, 215–229, doi:10.1023/A:1017532411978.

Chappell, N. A., W. Tych, A. Chotai, K. Bidin, W. Sinun, and T. H. Chiew (2006), BARUMODEL: Combined data based mechanistic models of runoff response in a managed rainforest catchment, *For. Ecol. Manage.*, *224*, 58–80, doi:10.1016/j.foreco.2005.12.008.

Clapp, R. B., and G. M. Hornberger (1978), Empirical equations for some soil hydraulic properties, *Water Resour. Res.*, *14*(4), 601–604, doi:10.1029/WR014i004p00601.

D'Odorico, P., L. Ridolfi, A. Porporato, and I. Rodríguez-Iturbe (2000), Preferential states of seasonal soil moisture: The impact of climate fluctuations, *Water Resour. Res.*, *36*(8), 2209–2219, doi:10.1029/2000WR900103.

Douglas, I., K. Bidin, G. Balamurugan, N. A. Chappell, R. P. D. Walsh, T. Greer, and W. Sinun (1999), The role of extreme events in the impacts of selective tropical forestry on erosion during harvesting and recovery phases at Danum Valley, Sabah, *Philos. Trans. R. Soc. London, Ser. B*, *354*, 1749–1761, doi:10.1098/rstb.1999.0518.

Field, C. B., M. J. Behrenfeld, J. T. Randerson, and P. Falkowski (1998), Primary production of the biosphere: Integrating terrestrial and oceanic components, *Science*, *281*, 237–240, doi:10.1126/science.281.5374.237.

Fisher, R. A., M. Williams, A. Lola da Costa, Y. Malhi, R. F. da Costa, S. Almeida, and P. Meir (2007), The response of an eastern Amazonian rain forest to drought stress: Results and modelling analyses from a throughfall exclusion experiment, *Global Change Biol.*, *13*, 2361–2378, doi:10.1111/j.1365-2486.2007.01417.x.

Food and Agriculture Organization of the United Nations (2005), Global Forest Resources Assessment 2005: Progress towards sustainable forest management, *FAO For. Pap.*, 147, Rome.

Giambelluca, T. W., J. Fox, S. Yarnasarn, P. Onibutr, and M. A. Nullet (1999), Dry-season radiation balance of land covers replacing forest in northern Thailand, *Agric. For. Meteorol.*, *95*, 53–65, doi:10.1016/S0168-1923(99)00016-7.

Giambelluca, T. W., A. D. Ziegler, M. A. Nullet, D. M. Truong, and L. T. Tran (2003), Transpiration in a small tropical forest patch, *Agric. For. Meteorol.*, *117*, 1–22, doi:10.1016/S0168-1923(03)00041-8.

Houghton, R. A., and J. L. Hackler (1999), Emissions of carbon from forestry and land-use change in tropical Asia, *Global Change Biol.*, *5*, 481–492, doi:10.1046/j.1365-2486.1999.00244.x.

Kanae, S., T. Oki, and K. Musiake (2001), Impact of deforestation on regional precipitation over the Indochina Peninsula, *J. Hydrometeorol.*, *2*, 51–70, doi:10.1175/1525-7541(2001)002<0051:IODORP>2.0.CO;2.

Katul, G., A. Porporato, and R. Oren (2007), Stochastic dynamics of plant-water interactions, *Annu. Rev. Ecol. Evol. Syst.*, *38*, 767–791, doi:10.1146/annurev.ecolsys.38.091206.095748.

Komatsu, H., N. Yoshida, H. Takizawa, I. Kosaka, C. Tantasirin, and M. Suzuki (2003), Seasonal trend in the occurrence of nocturnal drainage flow on a forested slope under a tropical monsoon climate, *Boundary Layer Meteorol.*, *106*, 573–592, doi:10.1023/A:1021202522995.

Kondo, J., and J. Xu (1997), Seasonal variations in the heat and water balances for nonvegetated surfaces, *J. Appl. Meteorol.*, *36*, 1676–1695, doi:10.1175/1520-0450(1997)036<1676:SVITHA>2.0.CO;2.

Kumagai, T., G. G. Katul, A. Porporato, T. M. Saitoh, M. Ohashi, T. Ichie, and M. Suzuki (2004a), Carbon and water cycling in a Bornean tropical rainforest under current and future climate scenarios, *Adv. Water Resour.*, *27*, 1135–1150, doi:10.1016/j.advwatres.2004.10.002.

Kumagai, T., G. G. Katul, T. M. Saitoh, Y. Sato, O. J. Manfroi, T. Morooka, T. Ichie, K. Kuraji, M. Suzuki, and A. Porporato (2004b), Water cycling in a Bornean tropical rain forest under current and projected precipitation scenarios, *Water Resour. Res.*, *40*, W01104, doi:10.1029/2003WR002226.

Kumagai, T., T. M. Saitoh, Y. Sato, T. Morooka, O. J. Manfroi, K. Kuraji, and M. Suzuki (2004c), Transpiration, canopy conductance and the decoupling coefficient of a lowland mixed dipterocarp forest in Sarawak, Borneo: Dry spell effects, *J. Hydrol.*, *287*, 237–251, doi:10.1016/j.jhydrol.2003.10.002.

Kumagai, T., T. M. Saitoh, Y. Sato, H. Takahashi, O. J. Manfroi, T. Morooka, K. Kuraji, M. Suzuki, T. Yasunari, and H. Komatsu (2005), Annual water balance and seasonality of evapotranspiration in a Bornean tropical rainforest, *Agric. For. Meteorol.*, *128*, 81–92, doi:10.1016/j.agrformet.2004.08.006.

Kumagai, T., T. Ichie, M. Yoshimura, M. Yamashita, T. Kenzo, T. M. Saitoh, M. Ohashi, M. Suzuki, T. Koike, and H. Komatsu (2006), Modeling CO_2 exchange over a Bornean tropical rain forest using measured vertical and horizontal variations in leaf-level physiological parameters and leaf area densities, *J. Geophys. Res.*, *111*, D10107, doi:10.1029/2005JD006676.

Kume, T., H. Takizawa, N. Yoshifuji, K. Tanaka, N. Tanaka, C. Tantasirin, and M. Suzuki (2007), Impact of soil drought on sap flow and water status of evergreen trees in a tropical monsoon forest in northern Thailand, *For. Ecol. Manage.*, *229*, 333–339.

Kuraji, K., P. Kowit, and M. Suzuki (2001), Altitudinal increase in rainfall in Mae Chaem watershed, Thailand, *J. Meteorol. Soc. Jpn.*, *79*, 353–363, doi:10.2151/jmsj.79.353.

Laio, F., A. Porporato, C. P. Fernandez-Illescas, and I. Rodríguez-Iturbe (2001a), Plants in water-controlled ecosystems: Active role in hydrologic processes and response to water stress: IV. Discussion of real cases, *Adv. Water Resour.*, *24*, 745–762, doi:10.1016/S0309-1708(01)00007-0.

Laio, F., A. Porporato, L. Ridolfi, and I. Rodríguez-Iturbe (2001b), Plants in water-controlled ecosystems: Active role in hydrologic processes and response to water stress: II. Probabilistic soil moisture dynamics, *Adv. Water Resour.*, *24*, 707–723, doi:10.1016/S0309-1708(01)00005-7.

Laurance, W. F. (1999), Reflections on the tropical deforestation crisis, *Biol. Conserv.*, *91*, 109–117, doi:10.1016/S0006-3207(99)00088-9.

Lean, J., and D. A. Warrilow (1989), Simulation of the regional climatic impact of Amazonian deforestation, *Nature*, *342*, 411–413, doi:10.1038/342411a0.

Mabuchi, K., Y. Sato, and H. Kida (2005a), Climatic impact of vegetation change in the Asian tropical region: part I. Case of the Northern Hemisphere summer, *J. Clim.*, *18*, 410–428, doi:10.1175/JCLI-3273.1.

Mabuchi, K., Y. Sato, and H. Kida (2005b), Climatic impact of vegetation change in the Asian tropical region: part II. Case of the Northern Hemisphere winter and impact on the extratropical circulation, *J. Clim.*, *18*, 429–446, doi:10.1175/JCLI-3274.1.

Malhi, Y., and J. Grace (2000), Tropical forests and atmospheric carbon dioxide, *Trends Ecol. Evol.*, *15*, 332–337, doi:10.1016/S0169-5347(00)01906-6.

Malhi, Y., and J. Wright (2004), Spatial patterns and recent trends in the climate of tropical rainforest regions, *Philos. Trans. R. Soc. London, Ser. B*, *359*, 311–329, doi:10.1098/rstb.2003.1433.

Manfroi, O. J., K. Kuraji, M. Suzuki, N. Tanaka, T. Kume, M. Nakagawa, T. Kumagai, and T. Nakashizuka (2006), Comparison of conventionally observed interception evaporation in a 100-m^2 subplot with that estimated in a 4-ha area of the same Bornean lowland tropical forest, *J. Hydrol.*, *329*, 329–349, doi:10.1016/j.jhydrol.2006.02.020.

Martínez-Vilalta, J., and J. Piñol (2002), Drought-induced mortality and hydraulic architecture in pine populations of the NE Iberian Peninsula, *For. Ecol. Manage.*, *161*, 247–256, doi:10.1016/S0378-1127(01)00495-9.

Martínez-Vilalta, J., J. Piñol, and K. Beven (2002), A hydraulic model to predict drought-induced mortality in woody plants: An application to climate change in the Mediterranean, *Ecol. Modell.*, *155*, 127–147, doi:10.1016/S0304-3800(02)00025-X.

Melillo, J. M., A. D. McGuire, D. W. Kicklighter, B. Moore III, C. J. Vorosmarty, and A. L. Schloss (1993), Global climate change and terrestrial net primary production, *Nature*, *363*, 234–240, doi:10.1038/363234a0.

Miller, G. R., D. D. Baldocchi, B. E. Law, and T. Meyers (2007), An analysis of soil moisture dynamics using multi-year data from a network of micrometeorological observation sites, *Adv. Water Resour.*, *30*, 1065–1081, doi:10.1016/j.advwatres.2006.10.002.

Nakagawa, M., et al. (2000), Impact of severe drought associated with the 1997–1998 El Niño in a tropical forest in Sarawak, *J. Trop. Ecol.*, *16*, 355–367, doi:10.1017/S0266467400001450.

National Park, Wildlife and Plant Conservation Department (2000), Preliminary forest land use assessment in 2000, R. For. Dep. of Thailand, Bangkok. (Available at http://www.forest.go.th/stat/stat_th.htm)

Nepstad, D. C., C. R. de Carvalho, E. A. Davidson, P. H. Jipp, P. A. Lefebvre, G. H. Negreiros, E. D. da Silva, T. A. Stone, S. E. Trumbore, and S. Vieira (1994), The role of deep roots in the hydrological and carbon cycles of Amazonian forests and pastures, *Nature*, *372*, 666–669, doi:10.1038/372666a0.

Nobre, C. A., P. J. Sellers, and J. Shukla (1991), Amazonian deforestation and regional climate change, *J. Clim.*, *4*, 957–988, doi:10.1175/1520-0442(1991)004<0957:ADARCC>2.0.CO;2.

O'Grady, A. P., D. Eamus, and L. B. Hutley (1999), Transpiration increases during the dry season: Patterns of tree water use in eucalypt open-forests of northern Australia, *Tree Physiol.*, *19*, 591–597.

Pockman, W. T., and J. S. Sperry (2000), Vulnerability to xylem cavitation and the distribution of Sonoran Desert vegetation, *Am. J. Bot.*, *87*, 1287–1299, doi:10.2307/2656722.

Porporato, A., F. Laio, L. Ridolfi, and I. Rodríguez-Iturbe (2001), Plants in water-controlled ecosystems: Active role in hydrologic processes and response to water stress: III. Vegetation water stress, *Adv. Water Resour.*, *24*, 725–744, doi:10.1016/S0309-1708(01)00006-9.

Porporato, A., P. D'Odorico, F. Laio, L. Ridolfi, and I. Rodríguez-Iturbe (2002), Ecohydrology of water-controlled ecosystems, *Adv. Water Resour.*, *25*, 1335–1348, doi:10.1016/S0309-1708(02)00058-1.

Priestley, C. H. B., and R. J. Taylor (1972), On the assessment of surface heat flux and evaporation using large-scale parameters, *Mon. Weather Rev.*, *100*, 81–92, doi:10.1175/1520-0493(1972)100<0081:OTAOSH>2.3.CO;2.

Rodríguez-Iturbe, I., and A. Porporato (2004), *Ecohydrology of Water-Controlled Ecosystems: Soil Moisture and Plant Dynamics*, Cambridge Univ. Press, New York.

Rodríguez-Iturbe, I., A. Porporato, L. Ridolfi, V. Isham, and D. R. Cox (1999), Probabilistic modelling of water balabce at a point: The role of climate, soil and vegetation, *Proc. R. Soc. London, Ser. A*, *455*, 3789–3805, doi:10.1098/rspa.1999.0477.

Rodríguez-Iturbe, I., A. Porporato, F. Laio, and L. Ridolfi (2001), Plants in water-controlled ecosystems: Active role in hydrologic processes and response to water stress: I. Scope and general outline, *Adv. Water Resour.*, *24*, 697–705, doi:10.1016/S0309-1708(01)00004-5.

Sperry, J. S. (2000), Hydraulic constraints on plant gas exchange, *Agric. For. Meteorol.*, *104*, 13–23, doi:10.1016/S0168-1923(00)00144-1.

Sperry, J. S., U. G. Hacke, R. Oren, and J. P. Comstock (2002), Water deficits and hydraulic limits to leaf water supply, *Plant Cell Environ.*, *25*, 251–263, doi:10.1046/j.0016-8025.2001.00799.x.

Tanaka, K., H. Takizawa, N. Tanaka, I. Kosaka, N. Yoshifuji, C. Tantasirin, S. Piman, M. Suzuki, and N. Tangtham (2003), Transpiration peak over a hill evergreen forest in northern Thailand in the late dry season: Assessing the seasonal changes in evapotranspiration using a multilayer model, *J. Geophys. Res.*, *108*(D17), 4533, doi:10.1029/2002JD003028.

Tanaka, K., H. Takizawa, T. Kume, J. Xu, C. Tantasirin, and M. Suzuki (2004), Impact of rooting depth and soil hydraulic properties on the transpiration peak of an evergreen forest in northern Thailand in the late dry season, *J. Geophys. Res.*, *109*, D23107, doi:10.1029/2004JD004865.

Tanaka, N., T. Kume, N. Yoshifuji, K. Tanaka, H. Takizawa, K. Shiraki, C. Tantasirin, N. Tangtham, and M. Suzuki (2008), A review of evapotranspiration estimates from tropical forests in Thailand and adjacent regions, *Agric. For. Meteorol.*, *148*, 807–819, doi:10.1016/j.agrformet.2008.01.011.

Timmermann, A., J. Oberhuber, A. Bacher, M. Esch, M. Latif, and E. Roeckner (1999), Increased El Niño frequency in a climate model forced by future greenhouse warming, *Nature*, *398*, 694–697, doi:10.1038/19505.

Tyree, M. T., and M. H. Zimmermann (2002), *Xylem Structure and the Ascent of Sap*, 2nd ed., Springer, Berlin.

Vincke, C., and Y. Thiry (2008), Water table is a relevant source for water uptake by a Scots pine (*Pinus sylvestris* L.) stand: Evidences from continuous evapotranspiration and water table monitoring, *Agric. For. Meteorol.*, *148*, 1419–1432, doi:10.1016/j.agrformet.2008.04.009.

World Resources Institute (2007), *EarthTrends: Environmental Information*, Washington, D. C. (Available at http://earthtrends.wri.org)

Yoshifuji, N., T. Kumagai, K. Tanaka, N. Tanaka, H. Komatsu, M. Suzuki, and C. Tantasirin (2006), Inter-annual variation in growing season length of a tropical seasonal forest in northern Thailand, *For. Ecol. Manage.*, *229*, 333–339, doi:10.1016/j.foreco.2006.04.013.

Zhang, Y., T. Li, B. Wang, and G. Wu (2002), Onset of the summer monsoon over the Indochina Peninsula: Climatology and interannual variations, *J. Clim.*, *15*, 3206–3221, doi:10.1175/1520-0442(2002)015<3206:OOTSMO>2.0.CO;2.

T. Kumagai and N. Yoshifuji, Kasuya Research Forest, Kyushu University, 394 Tsubakuro, Sasaguri-machi, Kasuya-gun 811-2415, Japan. (kuma@forest.kyushu-u.ac.jp)

T. Kume, School of Forestry and Resource Conservation, National Taiwan University, Taipei 10617, Taiwan.

M. Suzuki, Graduate School of Agricultural and Life Sciences, University of Tokyo, Tokyo 113-8657, Japan.

N. Tanaka, University Forest in Aichi, Graduate School of Agriculture and Life Sciences, University of Tokyo, Seto 489-0031, Japan.